International Conference on Mathematics, Computational Methods & Reactor Physics (M&C 2009)
Saratoga Springs, New York, May 3-7, 2009, on CD-ROM, American Nuclear Society, LaGrange Park, IL (2009)

Stochastic Methods for Uncertainty Quantification in Radiation Transport

[†]Erin D. Fichtl, [‡]Anil K. Prinja and [†]James S. Warsa

[†]Los Alamos National Laboratory
Computational Physics and Methods Group
Los Alamos, NM 87545
efichtl@lanl.gov;warsa@lanl.gov

[‡]Department of Chemical and Nuclear Engineering
University of New Mexico
Albuquerque, NM 87131
prinja@unm.edu

ABSTRACT

The use of generalized polynomial chaos (gPC) expansions is investigated for uncertainty quantification in radiation transport. The gPC represents second-order random processes in terms of an expansion of orthogonal polynomials of random variables and is used to represent the uncertain input(s) and unknown(s). We assume a single uncertain input—the total macroscopic cross section—although this does not represent a limitation of the approaches considered here. Two solution methods are examined: The Stochastic Finite Element Method (SFEM) and the Stochastic Collocation Method (SCM). The SFEM entails taking Galerkin projections onto the orthogonal basis, which, for fixed source problems, yields a linear system of fully-coupled equations for the PC coefficients of the unknown. For k-eigenvalue calculations, the SFEM system is non-linear and a Newton-Krylov method is employed to solve it. The SCM utilizes a suitable quadrature rule to compute the moments or PC coefficients of the unknown(s), thus the SCM solution involves a series of independent deterministic transport solutions. The accuracy and efficiency of the two methods are compared and contrasted. The PC coefficients are used to compute the moments and probability density functions of the unknown(s), which are shown to be accurate by comparing with Monte Carlo results. Our work demonstrates that stochastic spectral expansions are a viable alternative to sampling-based uncertainty quantification techniques since both provide a complete characterization of the distribution of the flux and the k-eigenvalue. Furthermore, it is demonstrated that, unlike perturbation methods, SFEM and SCM can handle large parameter uncertainty.

Key Words: Radiation Transport, Uncertainty Quantification, Polynomial Chaos Expansions

1. INTRODUCTION

We explore the use of stochastic transport formulations to quantify the uncertainty in the particle flux and, if fission is present, the k-eigenvalue, resulting from random uncertainties in input parameters such as cross sections. Given a stochastic representation of the input parameter, solution of the transport equation yields a stochastic characterization of the unknown(s) from which quantitative measures of output uncertainty (standard deviations, cumulative and probability density functions) can, in principle, be obtained. Sampling-based methods, where solutions are generated for individual realizations of the input parameters to construct a statistically significant sample space of outputs, are the easiest to implement but are also

computationally the most expensive. For practical computational purposes, the infinite dimensional probability space setting of phase-space random processes such as the particle flux must be replaced by a finite dimensional space using appropriate dimension reducing techniques.

Truncated spectral representations of random inputs and outputs in terms of random orthogonal basis functions, particularly the so-called polynomial chaos expansions [3, 11], are powerful dimension reducing methods that are endowed with strong convergence properties which enables high accuracy to be achieved at much lower cost than sampling methods. The problem then reduces to developing and solving a finite number of deterministic equations for the expansion coefficients. In this work, we contrast two different stochastic projection methods to obtain the equations for the expansion coefficients: (i) Galerkin projection, also known as the stochastic finite element method (SFEM), which leads to a system of coupled transport-like equations, and (ii) averaging by standard or specially constructed quadrature rules, also known as the stochastic collocation method (SCM), which leads to independent transport equations. The SFEM and SCM approaches are widely used in modeling system response to random parametric excitations in diverse applications [1, 3, 5, 10, 11] but have been largely overlooked in radiation transport applications (see, however [2, 9]).

Our goal is to develop these methods for quite general random variations in physical parameters for both fixed source and k-eigenvalue calculations. The stochastic spectral approach is demonstrated on a one group transport problem with a single random cross section that has a prescribed probability distribution. Application to both the fixed source and the k-eigenvalue problems is demonstrated. After a brief discussion of the polynomial chaos expansion of random processes, the SFEM and SCM methods are applied to a specific transport problem. Numerical results are then presented for the mean, standard deviation and probability distribution of the scalar flux or k-eigenvalue.

2. POLYNOMIAL CHAOS EXPANSIONS

Wiener [8] first demonstrated rigorously that any second-order random process could be expanded in a convergent sequence of Gaussian random variables using multidimensional Hermite polynomials as a basis and named this representation “Homogeneous Chaos”. Much later this expansion made possible the numerical computation of the response of complex physical systems to Gaussian distributed random excitations in model parameters and inputs, and culminated in the stochastic finite element method (SFEM) of Ghanem and Spanos [3]. Xiu and Karniadakis [11] subsequently extended this approach to allow a broader class of orthogonal polynomial bases and developed the so-called “generalized Polynomial Chaos” (gPC) expansion. They specifically showed, in the context of structural mechanics and CFD applications, that if the distribution function of the excitation was identical to the weight function of a classical orthogonal polynomial belonging to the Askey family [4], then a generalized expansion constructed from these random polynomials was convergent and the SFEM method could be readily adapted to handle uncertainty distributions other than Gaussian. The Askey scheme, along with their corresponding random variable distributions and support, are listed in Table I. As can be seen, the gPC of the Hermite type reduces to Wiener’s original homogeneous chaos.

If I_p are Askey polynomials of order p and ζ_{i_p} are their corresponding random variables, the gPC expansion of a second-order random process indexed by phase space coordinates $\vec{q}$ is given

Table I. Continuous Wiener-Askey Polynomial Chaoses and their Underlying Random Variables and Corresponding Weight Functions

Wiener-Askey Chaos $\{\Phi(\zeta)\}$	Random Variables ζ	Weight Function $w(\zeta)$	Support
Hermite	Gaussian	$\frac{1}{\sqrt{2\pi}}e^{-\frac{\zeta^2}{2}}$	$(-\infty,\infty)$
Laguerre	gamma	$\frac{\zeta^{\alpha-1}e^{-\zeta}}{\Gamma(\alpha)}$	$[0,\infty)$
Jacobi	beta	$\frac{\Gamma(\alpha+\beta+2)(1-\zeta)^{\alpha}(1+\zeta)^{\beta}}{2^{\alpha+\beta}(b-a)\Gamma(\alpha+1)\Gamma(\beta+1)}$	$[a,b]$
Legendre	uniform	$\frac{1}{(b-a)}$	$[a,b]$

by [11]:

$$\begin{aligned}\chi(\vec{q},\omega) = c_0(\vec{q})I_0 &+ \sum_{i_1=1}^{K} c_{i_1}(\vec{q})I_1(\zeta_{i_1}) \\ &+ \sum_{i_1=1}^{K}\sum_{i_2=1}^{i_1} c_{i_1 i_2}(\vec{q})I_2(\zeta_{i_1},\zeta_{i_2}) + \dots \\ &+ \sum_{i_1=1}^{K}\cdots\sum_{i_P=1}^{i_{P-1}} c_{i_1\dots i_P}(\vec{q})I_P(\zeta_{i_1},\dots,\zeta_{i_P}) \end{aligned} \tag{1}$$

where ω denotes a member of the random event space, or a realization and $c_{i_1\dots i_P}(\vec{q})$ are deterministic expansion coefficients that carry the phase space dependence. This expansion can be rewritten in a more compact notation as

$$\chi(\omega) = \sum_{i=0}^{M} \hat{c}_i(\vec{q})\Phi_i(\{\zeta_r\}). \tag{2}$$

where the $\hat{c}_i(\vec{q})$ and $\Phi_i(\{\zeta_r\})$ denote various combinations of $c_{i_1\dots i_p}$ and $I_p(\zeta_{i_1},\dots,\zeta_{i_p})$. Invoking the orthogonality of the basis functions, the expansion coefficients in Eq. 2 are given by:

$$\hat{c}_j(\vec{q}) = \frac{\langle \chi, \Phi_j(\zeta)\rangle}{\langle \Phi_j^2(\zeta)\rangle} \tag{3}$$

where we have introduced the inner product

$$\langle f(\zeta), g(\zeta)\rangle = \int f(\zeta)g(\zeta)w(\zeta)d\zeta. \tag{4}$$

The weight function $w(\zeta)$ in the above definition of the inner product is the weight function associated with the particular choice of Askey polynomials used. As, by definition, it is also the probability distribution function for the random variable, it follows that the inner product $\langle f(\zeta), g(\zeta)\rangle$ is equivalent to the mathematical expectation of $f(\zeta)\,g(\zeta)$.

3. APPLICATION OF GPC TO THE TRANSPORT EQUATION

3.1. Fixed Source Problem

We now apply the gPC method to a steady-state, mono-energetic, fixed source homogeneous medium transport problem with a random total cross section. The appropriate random transport equation is given by:

$$\mu\frac{\partial\psi(x,\mu;\omega)}{\partial x}+\sigma(\omega)\psi(x,\mu;\omega)=\sigma(\omega)\,\frac{c}{2}\phi(x;\omega)+Q(x,\mu) \tag{5}$$

where $\psi(x,\mu;\omega)$ is the random angular flux and otherwise standard notation is used. Appropriate boundary conditions on the free surfaces are assumed. The uncertain input parameter is assumed to be the total cross section, with a known probability distribution function belonging to the Askey scheme, and the mean number of secondaries c is assumed nonrandom. Thus we are assuming that the uncertainty exists only in the atomic density. This model of input randomness is adopted here for illustration only and does not constitute a limitation of the approach. The angular flux and total cross section are first expanded in terms of the appropriate random polynomials, the gPC expansion, formally expressed as:

$$\psi(x,\mu;\omega) = \sum_{i=0}^{P}\psi_i(x,\mu)\Phi_i(\zeta(\omega)) \tag{6a}$$

$$\sigma(\omega) = \sum_{j=0}^{P_\sigma}\sigma_j\Phi_j(\zeta(\omega)), \tag{6b}$$

where σ_j is known since the distribution of the cross section is known and the expansion coefficients $\psi_i(x,\mu)$ represent deterministic unknowns. We describe two approaches for obtaining equations for these coefficients. In one, the gPC expansion given in Eqs. 6 is first substituted into the transport equation:

$$\mu\sum_{i=0}^{P}\frac{\partial\psi_i(x,\mu)}{\partial x}\Phi_i(\zeta(\omega))+\sum_{i=0}^{P}\sum_{j=0}^{P_\sigma}\psi_i(x,\mu)\sigma_j\Phi_i(\zeta(\omega))\Phi_j(\zeta(\omega))= \frac{c}{2}\sum_{i=0}^{P}\sum_{j=0}^{P_\sigma}\phi_i(x)\sigma_j\Phi_i(\zeta(\omega)\Phi_j(\zeta(\omega))+Q(x,\mu). \tag{7}$$

Projections are then taken over suitable test functions to eliminate the random functions. This procedure then yields the closed system of equations for the expansion coefficients ψ_ℓ, $\ell=0,1,\ldots P$:

$$\mu\frac{\partial\psi_\ell}{\partial x}+\sum_{i=0}^{P}b_{\ell i}\psi_i=\frac{c}{2}\sum_{i=0}^{P}b_{\ell i}\phi_i+q_\ell,\qquad \ell=0,1,\ldots,P \tag{8}$$

where $b_{\ell i}=\sum_{j=0}^{P_\sigma}\sigma_j\frac{\langle\Phi_i\Phi_j\Phi_\ell\rangle}{\langle\Phi_\ell^2\rangle}$ and $q_\ell=\frac{\langle\Phi_\ell Q\rangle}{\langle\Phi_\ell^2\rangle}=\delta_{\ell 0}Q$. In view of the use of basis expansions and projections over test functions in the random dimension, this approach is commonly referred to as the stochastic finite element method or SFEM. It's use enables a stochastic transport equation to

be reduced to a system of $(P+1)$ fully-coupled deterministic equations for the expansion coefficients $\psi_\ell(x,\mu)$. As Eq. 8 resembles a system of coupled transport equations, not unlike multigroup equations, standard numerical methods, direct or iterative, can presumably be employed for numerical solution. Of interest then is the order P of the expansion that is necessary to accurately describe the solution of the original random problem, with accuracy determined in the sense of convergence of ensemble averages of the flux and/or its probability distribution.

An alternative approach to obtaining the expansion coefficients in Eq. 6a is to use quadrature to evaluate the projections over the gPC polynomials. If the weight functions correspond to classical orthogonal polynomials listed in Table I, appropriate Gaussian quadrature sets are available or can be constructed to compute the projections with potentially high accuracy. From Eq. 3, we then have for the ℓ^{th} moment of the flux:

$$\psi_\ell = \frac{\langle \psi,\, \Phi_\ell \rangle}{\langle \Phi_\ell^2 \rangle} \approx \frac{1}{\langle \Phi_\ell^2 \rangle} \sum_{m=1}^{M} w_m \Phi_{\ell,m} \psi_m. \tag{9}$$

where $\psi_m(x,\mu)$ is the angular flux corresponding to a deterministic value of the cross section σ_m from the quadrature set appropriate to the cross section pdf, with w_m the associated weight and $\Phi_{\ell,m}$ the ℓ^{th} order polynomial evaluated at the m^{th} abscissa. Like the SFEM method presented earlier, the SCM method yields a deterministic transport problem but with the added advantage that the equations for the angular fluxes $\{\psi_m(x,\mu), m = 1, 2 \cdots M\}$ are uncoupled. This quadrature-based method of obtaining the coefficients is known as the Stochastic Collocation Method or SCM.

Once the expansion coefficients have been obtained by either method, statistical realizations of the angular flux can be generated by sampling the random polynomials in Eq. 6a. Ensemble averages such as the mean and the variance can be constructed either by taking appropriate projections of the gPC expansion

$$\langle \psi^n \rangle = \left\langle \left(\sum_{p=0}^{P} \psi_p(x,\mu) \Phi_p(\omega) \right)^n \right\rangle \tag{10}$$

where, from orthogonality of the basis functions Φ_p, we have, for instance, $\langle \psi \rangle = \psi_0$ and $\langle \psi^2 \rangle = \sum_{p=0}^{P} \psi_p^2(x,\mu) \langle \Phi_p^2(\omega) \rangle$, or directly by quadrature

$$\langle \psi^n(x,\mu) \rangle \approx \sum_{m=1}^{M} w_m \psi_m^n(x,\mu), n = 1, 2, \ldots \tag{11}$$

Finally, benchmark solutions were obtained by solving Eq. 5 for a large number of cross section realizations sampled from the total cross section pdf and performing suitable averages. As with the SCM method, this Monte Carlo approach yields independent transport equations but unlike the SCM method, all solutions are uniformly weighted in the averaging process.

In all three methods, the angular flux is approximated using the discrete ordinates or $\mathrm{S_N}$ method in angle and a linear discontinuous finite element representation in space. The resulting discretized system can be expressed as:

$$\mathbf{L}\vec{\psi} = \mathbf{MSD}\vec{\psi} + \vec{q} \tag{12}$$

where $\mathbf{L}$ is the streaming and removal operator, $\mathbf{M}$ is the moment-to-discrete operator, $\mathbf{S}$ is the scattering operator, $\mathbf{D}$ is the discrete-to-moment operator (i.e., $\mathbf{D}\vec{\psi} = \vec{\phi}$), $\vec{\psi} = \left[\vec{\psi}_0 \dots \vec{\psi}_P\right]^T$ and $\vec{q} = [\vec{q}_0 \dots \vec{q}_P]^T$. In the SFEM case, the system of equations can be solved using an inexact block Gauss-Seidel (IBGS) iteration in which there are $(P+1)$ blocks corresponding to the $(P+1)$ flux moments or using a Krylov iterative method which can be preconditioned using this splitting. The SCM involves solving a series of deterministic transport equations, which can be accomplished using standard source iteration or a Krylov iterative method.

3.2. k-Eigenvalue Problem

We now apply the gPC to a mono-energetic k-eigenvalue problem, where the total cross section is once again random:

$$\mu\frac{\partial\psi(x,\mu;\omega)}{\partial x} + \sigma(\omega)\psi(x,\mu;\omega) = \frac{\sigma(\omega)}{2}\left(c + \frac{\nu f}{k(\omega)}\right)\phi(x;\omega) \tag{13}$$

where f is defined such that $\sigma_f(\omega) = f\sigma(\omega)$ so that, once again, there is a single random input. Eqs. 6 are substituted into Eq. 13 along with the additional condition

$$\frac{1}{k(\omega)} = \lambda(\omega) \approx \sum_{j=0}^{P}\Phi_j\lambda_j \tag{14}$$

where k has been represented in terms of its inverse $\lambda = \frac{1}{k}$ in order to keep all of the basis functions in the numerator. This yields:

$$\mu\sum_{i=0}^{P}\Phi_i\frac{\partial\psi_i(x,\mu)}{\partial x} + \sum_{i=0}^{P}\sum_{j=0}^{P_\sigma}\Phi_i\Phi_j\left(\psi_i(x,\mu) - \frac{c}{2}\phi_i(x)\right)\sigma_j = \frac{\nu f}{2}\sum_{m=0}^{P}\sum_{i=0}^{P}\sum_{j=0}^{P_\sigma}\Phi_m\Phi_i\Phi_j\lambda_m\phi_i(x)\sigma_j \tag{15}$$

Taking a Galerkin projection onto the basis yields the following system of SFEM equations:

$$\mu\frac{\partial\psi_\ell}{\partial x} + \sum_{i=0}^{P}b_{\ell i}\left(\psi_i - \frac{c}{2}\phi_i\right) = \frac{\nu}{2}\sum_{m=0}^{P}\lambda_m\sum_{i=0}^{P}f_{\ell mi}\phi_i, \qquad \ell = 0,\dots,P \tag{16}$$

where $b_{\ell i} = \sum_{j=0}^{P_\sigma}\sigma_j\frac{\langle\Phi_\ell\Phi_i\Phi_j\rangle}{\langle\Phi_\ell^2\rangle}$ and $f_{\ell mi} = \sum_{j=0}^{P_\sigma}\frac{\langle\Phi_\ell\Phi_m\Phi_i\Phi_j\rangle}{\langle\Phi_\ell^2\rangle}\sigma_j$. Application of the angular and spatial discretization refashions Eq. 16 in the form of a matrix equation

$$\sum_{i=0}^{P}\left(\mathbf{L}_{\ell i} - \mathbf{M}\mathbf{S}_{\ell i}\mathbf{D}\right)\vec{\psi}_i = \sum_{m=0}^{P}\lambda_m\sum_{i=0}^{P}\mathbf{M}\mathbf{S}_{f,\ell mi}\mathbf{D}\vec{\psi}_i, \qquad \ell = 0,\dots,P \tag{17}$$

where $\mathbf{L}_{\ell i}$ is the streaming and removal operator, $\mathbf{M}$ is the moment-to-discrete operator, $\mathbf{S}_{\ell i}$ and $\mathbf{S}_{f,\ell mi}$ are the scattering and fission source matrices, respectively, and $\mathbf{D}$ is the discrete-to-moment operator. Thus, in total there are $2IN(P+1)$ equations, where I is the number of spatial cells and N is the number of quadrature angles, while the solution vector,

$$\vec{x} = [\vec{\psi}_0,\dots,\vec{\psi}_P,\lambda_0,\dots,\lambda_P]^T,$$

contains $(2IN+1)(P+1)$ unknowns. The additional $(P+1)$ equations can be obtained using the normalization condition on the eigenfunction:

$$\vec{\phi}^T\vec{\phi} = \left(\mathbf{D}\vec{\psi}\right)^T\left(\mathbf{D}\vec{\psi}\right) = 1 \tag{18}$$

where $\vec{\psi}$ is the exact eigenfunction and is a function of the random dimension. Since the norm of $\vec{\psi}$ is a deterministic quantity, Eq. 18 states that for *each realization* of the material, the L_2-norm of the eigenfunction vector is unity. The eigenfunction can then be replaced by its PC expansion to yield

$$\sum_{i=0}^{P}\sum_{j=0}^{P}\left(\mathbf{D}\vec{\psi}_i\right)^T\left(\mathbf{D}\vec{\psi}_j\right)\Phi_i\Phi_j = 1. \tag{19}$$

Projecting onto the basis then gives the final $(P+1)$ equations:

$$\sum_{i=0}^{P}\sum_{j=0}^{P}\left(\mathbf{D}\vec{\psi}_i\right)^T\left(\mathbf{D}\vec{\psi}_j\right)\langle\Phi_i\Phi_j\Phi_\ell\rangle = \delta_{\ell 0}, \qquad \ell = 0,\ldots,P. \tag{20}$$

As can be seen in Eq. 17, the matrix equation is non-linear since both the eigenvalue and the eigenfunction are unknown, therefore it is necessary to use a non-linear iterative solver such as Newton-Raphson. The system of equations is first written in the form

$$F(\vec{x}) = [F_0(\vec{x})\cdots F_P(\vec{x})F_{P+1}(\vec{x})]^T = 0$$

where $\vec{x}$ is the solution vector, and the F_ℓ are given by

$$F_\ell(\vec{x}) = \sum_{i=0}^{P}\left(\mathbf{L}_{\ell i} - \mathbf{M}\mathbf{S}_{\ell i}\mathbf{D}\right)\vec{\psi}_i - \sum_{m=0}^{P}\lambda_m\sum_{i=0}^{P}\mathbf{M}\mathbf{S}_{f,\ell m i}\mathbf{D}\vec{\psi}_i \tag{21a}$$

$$F_{P+1,\ell}(\vec{x}) = \sum_{i=0}^{P}\sum_{j=0}^{P}\left(\mathbf{D}\vec{\psi}_i\right)^T\left(\mathbf{D}\vec{\psi}_j\right)\langle\Phi_i\Phi_j\Phi_\ell\rangle - \delta_{\ell 0} \tag{21b}$$

for $\ell = 0,\ldots,P$. The iteration then takes the form

$$J\cdot\vec{\delta x}^{(z)} = -F(\vec{x}^{(z)}) \tag{22}$$

$$\vec{x}^{(z+1)} = \vec{x}^{(z)} + \vec{\delta x}^{(z)} \tag{23}$$

where z is the iteration index and $J_{ij} = \frac{\partial F_i}{\partial x_j}$.

Newton-Raphson shows quadratic convergence near the solution point, but can diverge if the initial guess is not sufficiently accurate. Here, the solution is initialized using SCM, although there are other possible intializing algorithms. It is also possible to compute the PC coefficients of k using SCM in the same manner that the PC coefficients of ψ were computed in Eq. 9.

4. NUMERICAL RESULTS

4.1. Fixed Source

To illustrate the stochastic spectral approach described above, we assume that the pdf of the total cross section is given by the two-parameter gamma distribution:

$$P(\sigma) = \frac{1}{\Gamma(\alpha)\beta^{\alpha}}\sigma^{\alpha-1}\exp\left(-\frac{\sigma}{\beta}\right) \tag{24}$$

We set $\alpha = 5$ and $\beta = 1$ so as to obtain a cross section mean of 5 cm^{-1} and a variance of 5 cm^{-2}. An attractive feature of this distribution is that the support is positive so that, unlike the Gaussian distribution, negative cross sections cannot arise. Also, as can be seen in Fig. 1, the pdf is unimodal and the parameters can be tuned to yield a symmetric or skewed distribution to cover a range of uncertainty models.

:

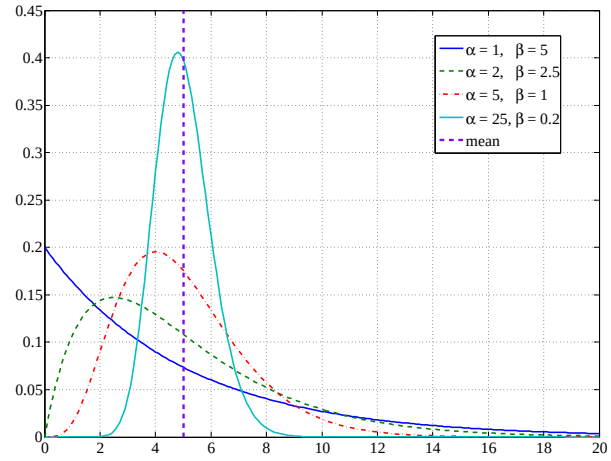

Figure 1. Gamma Distribution for Various Values of α and β

Shown in Fig. 2 are the mean and relative standard deviation of the scalar flux for an incident beam on the left face of a 5 cm slab. Results were computed using Monte Carlo for 3.8934×10^6 realizations to achieve a relative sample standard deviation of 1%, Gauss-Laguerre quadrature for various quadrature orders M, and SFEM with Laguerre chaos for various PC orders P. As can be seen, a PC order of P in SFEM is equivalent to a quadrature order of $M = (P + 1)$, a result that can be proven using matrix manipulation and numerical results, but which is not shown here. Although the mean scalar flux is seen to converge at $P = 7$ and $M = 8$, the standard deviation requires a higher order expansion or quadrature. A similar observation can be made for the pdf of the scalar flux, as shown in Fig. 2(b) for several depths, generated using both Monte Carlo and PC expansions. It is interesting to observe how rapidly the flux pdf becomes skewed with increasing depth into the slab, requiring an expansion order of $P = 31$ before the PC-generated distributions converge. The distributions also show a long tail for flux values considerably larger than the mean, which is the result of long neutron transmission paths created in realizations with lower

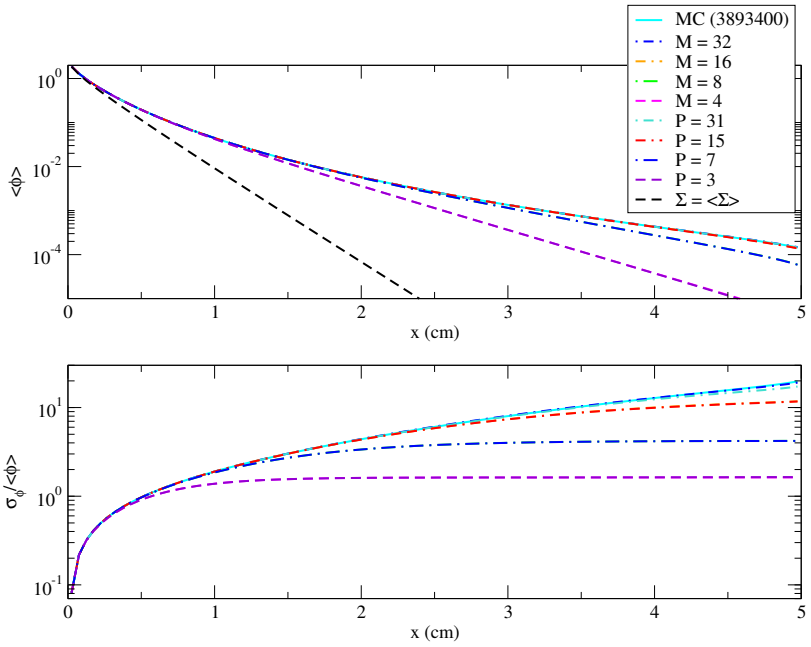

..

(a) flux

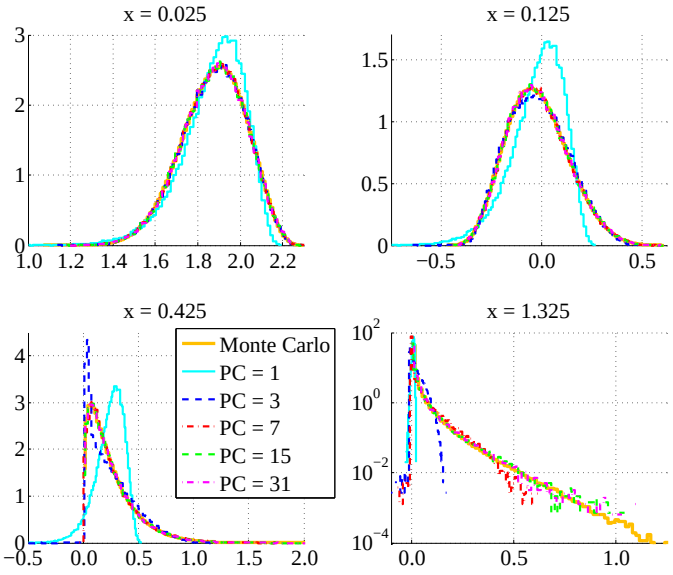

..

(b) pdf

Figure 2. Scalar Flux: SFEM with a Laguerre Chaos expansion and SCM with Gauss-Laguerre Quadrature ($\alpha = 5$, $\beta = 1$, $\langle\sigma\rangle = 5.0$ cm^{-1}, $v_\sigma = 5.0$ cm^{-2}, $c = 0.5$)

Table II. IBGS Iteration Count and Run Time in Seconds: Average over 25 Runs for a Gamma Distributed Cross Section for SFEM with Laguerre Chaos and SCM with Gauss-Laguerre Quadrature ($\alpha = 5$, $\epsilon = 10^{-9}$)

		Iteration Count			Run Time (s)		
c	P M	Richardson	GMRES(8)	BiCGStab	Richardson	GMRES(8)	BiCGStab
0.5	1 2	32 52	15 22	8 12	0.0116 0.0072	0.014 0.0088	0.0116 0.0076
	3 4	54 104	25 43	13 25	0.0472 0.0144	0.052 0.018	0.0444 0.0156
	7 8	112 208	52 83	32 49	0.288 0.0304	0.2492 0.036	0.2432 0.0316
	15 16	242 415	112 158	62 92	1.6896 0.0624	1.352 0.0732	1.1996 0.064
	31 32	466 827	199 298	NC 174	9.214 0.138	6.372 0.151	NC 0.135
0.99	1 2	1267 2321	117 198	51 60	0.4424 0.302	0.0976 0.0712	0.0628 0.0308
	3 4	1385 4674	201 397	89 141	1.1768 0.609	0.4004 0.143	0.272 0.0716
	7 8	1537 9531	338 752	158 293	3.8676 1.24	1.588 0.273	1.1628 0.15
	15 16	1529 19630	560 1450	217 618	10.3232 2.57	6.606 0.533	4.0132 0.321
	31 32	1516 40593	626 2700	NC 1229	29.9836 5.33	19.7056 0.999	NC 0.652

densities than average. Also, it will be noted that the flux appears to be nonrandom near the incident boundary, as reflected in the moments plot and the very peaked pdf plot. This can be attributed to the fact that the flux in 1D slab geometries depends only on the optical depth variable, into which all randomness is subsumed and which is zero at the surface. Moreover, for a thick slab such that the net transmission is small and hence the slab appears to be semi-infinite in extent, the surface angular flux in each realization can be shown to be nonrandom.

Table II shows iteration counts and run times given as an average over 25 runs for this same test case. An inexact block Gauss-Seidel splitting is employed and three different iteration schemes are tested: Richardson iteration and two Krylov methods, restarted generalized minimum residual (GMRES(n)) and bi-conjugate gradient stabilized (BiCGStab). For both SFEM and SCM, the iteration counts given are totals. Thus, for the SCM quadrature solution, the count is the total number of deterministic transport iterations for all quadrature abscissas. For the SFEM solution, the count is the total number of iterations for the coupled SFEM equations. As can be seen, larger iteration counts, hence larger run times, are required for larger scattering ratios, as expected in a

transport setting when the material becomes more diffusive. Since the SCM involves a series of deterministic transport computations, for which convergence is strongly influenced by the scattering ratio, the iteration count per quadrature point varies only slightly with quadrature order and variance and the run time per transport computation remains constant provided c does not change. On the other hand, for SFEM, the runtime per iteration more than doubles each time the number of PC coefficients doubles. Although there are always fewer SFEM iterations than SCM iterations, each SFEM iteration involves inverting a much larger matrix, and is therefore more computationally extensive. Therefore, without exception, an M-term SCM quadrature solution always runs in a shorter time than an SFEM solution for $P = (M - 1)$. Since these solutions are equivalent, SCM is shown to be the more efficient solution method when there is a single random variable.

4.2. k-Eigenvalue

Numerical results were obtained for a critical reactor with uncertain macroscopic cross sections. The test problem was taken from an analytical benchmark test set originally intended for criticality code verification [7]. The system is a bare slab reactor composed of uranium dioxide with material parameters $\nu = 1.70$, $\sigma_f = 0.054628$ cm^{-1}, $\sigma_c = 0.027314$ cm^{-1}, $\sigma_s = 0.464338$ cm^{-1} and $\sigma_t = 0.54628$ cm^{-1}. The analytic critical size of the reactor is given as 20.74213 cm in [7]. Using 100 spatial cells and 32 discrete ordinates, by trial and error the critical size was found to be 20.742942196391 cm. Using this critical size and the mean cross sections listed previously, the total cross section is assumed to be randomly distributed according to a known pdf.

Table III. Iteration Counts, Run Times and Errors for the SCM and a Single SCM-initialized SFEM Iteration in a Multiplying Material: Uniform Random Variable and Legendre Chaos (SCM tolerance = 10^{-6})

		SCM Initialize				SFEM		
$\frac{\sqrt{v_\sigma}}{\langle\sigma\rangle}$	PC	M	GMRES(8)	run time (s)	$\| \mathrm{F_{SCM}} \|_2$	GMRES(25)	run time (s)	$\| \mathrm{F_{SFEM}} \|_2$
$\frac{1}{5}$	1	2	102	0.217	3.2355e-04	20	0.723875	2.6288e-07
	3	4	211	0.45	3.0228e-04	39	5.9535	2.3297e-07
	7	8	420	0.904	3.2456e-04	90	60.283	2.5748e-07
	15	16	847	1.8	3.2652e-04	125	536.956	1.9739e-07
$\frac{1}{\sqrt{5}}$	1	2	108	0.228	2.2224e-03	21	0.7538	1.4410e-06
	3	4	214	0.457	1.3736e-03	98	9.4105	8.5795e-07
	7	8	433	0.924	4.3315e-04	187	130.33	4.8508e-07
	15	16	862	1.84	4.2298e-04	253	1148.068	5.2655e-07

We first compare the accuracy and computational efficiency of SCM-initialized Newton's method for SFEM and SCM for this problem. Table III shows iteration counts, run times and L_2-Norms of F for the SCM initialization and a single Newton-Krylov SFEM iteration. The SCM initialization produces a solution with $\| \mathrm{F_{SCM}} \|_2$ on the order of 10^{-3} or 10^{-4} in all cases. A single

:

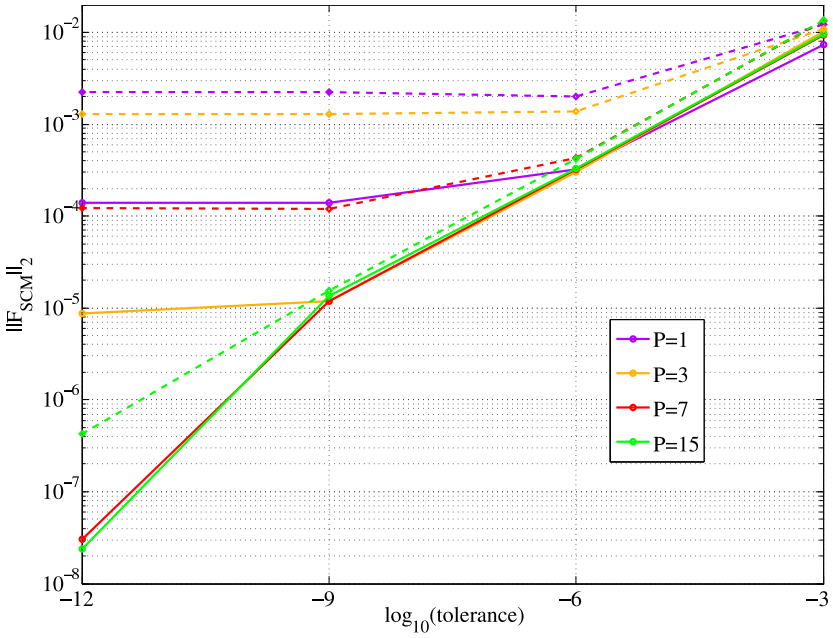

Figure 3. $\| \mathrm{F}_{\mathrm{SCM}} \|_2$ as a Function of Tolerance for Various PC Orders (Solid Lines: $\frac{\sqrt{v_\sigma}}{\langle\sigma\rangle} = \frac{1}{5}$, Dashed Lines: $\frac{\sqrt{v_\sigma}}{\langle\sigma\rangle} = \frac{1}{\sqrt{5}}$)

Newton-Krylov SFEM iteration then produces an $\| \mathrm{F}_{\mathrm{SFEM}} \|_2$ on the order of 10^{-6} or 10^{-7}. Note, however, that these are L_2 norms—the individual elements of $\mathrm{F}_{\mathrm{SCM}}$ and $\mathrm{F}_{\mathrm{SFEM}}$ are generally smaller than the norm.

In the previous section, it was shown that SCM using a quadrature order of M is equivalent to SFEM using a PC order of $P = (M - 1)$. The same cannot be said for multiplying media due to the non-linear nature of the SFEM equations. As can be seen in Fig. 3, the size of $\| \mathrm{F}_{\mathrm{SCM}} \|_2$ is strongly dependent on the tolerance set for the power iteration used to compute the k-eigenvalue and the inner source iteration used to compute the flux updates. For $\frac{\sqrt{v_\sigma}}{\langle\sigma\rangle} = \frac{1}{5}$, as the tolerance decreases, $\| \mathrm{F}_{\mathrm{SCM}} \|_2$ decreases as well and is on the order of 10^{-8} for a tolerance of 10^{-12} for $P = 7$ and 15. However, for $P = 1$ and 3, $\| \mathrm{F}_{\mathrm{SCM}} \|_2$ is approximately 10^{-4} and 10^{-5}, respectively. Even with a very small tolerance, $\| \mathrm{F}_{\mathrm{SCM}} \|_2$ is quite large for small P, indicating that SCM with a quadrature order of $M = (P + 1)$ is not in fact equivalent to SFEM with a PC order of P. (In comparison, consider that if σ_f and ν are set to zero and a volume source is placed in the system, SCM with a quadrature order of $M = (P + 1)$ yields $\| \mathrm{F}_{\mathrm{SCM}} \|_2$ on the order of 10^{-12} or 10^{-13} for $P = 1$, 3, 7 and 15.) However, the fact that $\| \mathrm{F}_{\mathrm{SCM}} \|_2$ gets very small for $P = 7$ as the tolerance gets small indicates that the solution is essentially converged and that the two methods do eventually converge to the same answer, as would be expected. Similar conclusions can be drawn for $\frac{\sqrt{v_\sigma}}{\langle\sigma\rangle} = \frac{1}{\sqrt{5}}$, although clearly the solution does not converge as quickly as it does for the smaller variance.

Table IV. Runtime for SCM for $M = (P+1)$ in seconds: Uniform Random Variable and Legendre Chaos ($\frac{\sqrt{v_\sigma}}{\langle\sigma\rangle} = \frac{1}{5}$)

tolerance	$P = 1$	$P = 3$	$P = 7$	$P = 15$
10^{-3}	0.08	0.16	0.39	0.64
10^{-6}	0.217	0.45	0.904	1.8
10^{-9}	0.36	0.76	1.44	2.9
10^{-12}	0.66	1.29	2.58	5.04

Table V. Gamma Distribution: Mean and standard deviation of the k-eigenvalue calculated using M-dimensional Gauss-Laguerre quadrature and Monte Carlo with 10^6 realizations ($\alpha = 5$, $\frac{\sqrt{v_\sigma}}{\langle\sigma\rangle} = \frac{1}{\sqrt{5}}$).

M (P)	2 (1)	4 (3)	8 (7)	16 (15)	32 (31)	Monte Carlo
mean	9.6224972e-01	9.5207180e-01	9.5190828e-01	9.5191928e-01	9.5191913e-01	9.5179068e-01
stdev	7.4869877e-02	1.1745105e-01	1.2343850e-01	1.2331635e-01	1.2331795e-01	1.2346672e-01

:

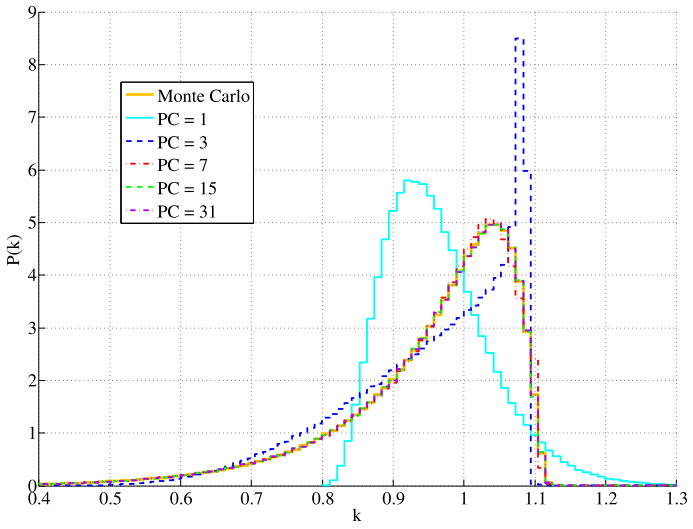

Figure 4. PDF of the k-eigenvalue: Laguerre Chaos expansion of the Gamma Distribution ($\frac{\sqrt{v_\sigma}}{\langle\sigma\rangle} = \frac{1}{\sqrt{5}}$)

In Table IV, run times are also shown for $\frac{\sqrt{v_\sigma}}{\langle\sigma\rangle} = \frac{1}{5}$ (run times are almost identical for $\frac{\sqrt{v_\sigma}}{\langle\sigma\rangle} = \frac{1}{\sqrt{5}}$ and are therefore not shown) for various tolerances and PC orders. Although it is much more expensive to use a smaller tolerance in SCM, it is not nearly as expensive as doing even a single SFEM Newton-Krylov iteration. Although doing that SFEM iteration does produce more accurate results for $P = 1$ and 3, these solutions are not converged therefore there is little point in doing the extra work.

Table V shows the mean and standard deviation of the k-eigenvalue computed using the PC coefficients of k, up to order P, which were computed using SCM with a quadrature order of $M = (P + 1)$. As can be seen, the SCM yields accurate results with respect to Monte Carlo and, as in the fixed source case, the mean converges for smaller gPC and SCM quadrature order than the standard deviation does. Fig. 4 shows the distribution of the k-eigenvalue for the same gamma distribution used in Fig. 2, albeit for a different β. The pdf was computed by sampling the random variable, computing k from its PC expansion and tabulating the results. As can be seen, the gPC agrees well with the Monte Carlo.

5. CONCLUSIONS

In applications for independent, uncorrelated random variables, such as those explored, the use of gPC expansions is shown to be efficient and effective. The SCM was also shown to be much more efficient than the SFEM, yielding comparable results for $M = (P + 1)$ at a fraction of the cost. In addition, the SCM requires a series of *independent* deterministic transport computations and can therefore be 'wrapped around' an existing transport code, requiring no modification to the tranport computation itself. SFEM, on the other hand, produces a coupled system of transport equations and its solution requires an entirely new algorithm. In multiplying media, the SFEM equations are nonlinear and even a single Newton-Krylov iteration is far more time-consuming than an SCM initialization, which can achieve a high level of accuracy quite cheaply.

The advantage to using gPC expansions to represent problem outputs is that those quantities can be completely characterized using the gPC coefficients. Thus, a relatively small dataset contains all of the information necessary to construct pdfs and cdfs, define responses of specific outputs to inputs, and compute statistical moments. In short, it is capable of producing the same results as sampling-based approaches and can additionally handle large uncertainties unlike the perturbation methods typically employed in nuclear applications for uncertainty quantification. The disadvantage is that, in order to extract anything more than the moments of the output, it is necessary to sample the random variables involved. Thus post-processing can be quite computationally demanding, although not as demanding as conducting a Monte Carlo simulation on the entire system. Furthermore, computationally demanding analyses such as risk assessments for nuclear reactors and the Department of Energy's nuclear waste repository in Yucca Mountain can require 10s to 100s of uncertain inputs, which may in addition be correlated [6]. As the number of dimensions increases, the number of quadrature points required by SCM and the number of terms in the gPC expansion increase rapidly. If the variables are correlated, it is possible to use principal component analysis to reduce the number of random variables. Even so, it may be that an optimized multi-dimensional sampling method such as Latin Hypercube, which is already in widespread use for problems of this sort, may be more efficient than SCM for large-scale applications. It would be enlightening to conduct an analysis on a real-world system

of this scale.

ACKNOWLEDGEMENTS

A portion of this research was performed under appointment to the U.S. Department of Energy Nuclear Engineering and Health Physics Fellowship Program sponsored by the U.S. Department of Energy's Office of Nuclear Energy, Science, and Technology.

REFERENCES

[1] I. Babuska, F. Nobile, and R. Tempone. A stochastic collocation method for elliptic partial differential equations with random input data. *SIAM Journal on Numerical Analysis*, 45(3):1005–1034, 2007.

[2] A.F. Emery. Some thoughts on solving the radiative transfer equation in stochastic media using polynomial chaos and wick products as applied to radiative equilibrium. *Journal of Quantitative Spectroscopy and Radiative Transfer*, 93(1-3):61–77, June 2005.

[3] R. Ghanem and P. Spanos. *Stochastic Finite Elements: A Spectral Approach*. Springer-Verlag, New York, 1991.

[4] R. Koekoek and R.F. Swarttouw. The askey-scheme of hypergeometric orthogonal polynomials and its q-analogue. Technical Report 94-05, TU Delft, Delft, The Netherlands, 1994.

[5] L. Mathelin, M.Y. Hussaini, and T.A. Zang. Stochastic approaches to uncertainty quantification in cfd simulations. *Numerical Algorithms*, 38(1-3):209–236, 2005.

[6] C.J. Sallaberry, J.C. Helton, and S.C. Hora. Extension of latin hypercube samples with correlated variables. *Reliability Engineering and System Safety*, 93(7):1047–1059, July 2008.

[7] A. Sood, R.A. Forster, and D.K. Parsons. Analytical benchmark test set for criticality code verification. *Progress in Nuclear Energy*, 42(1):55–106, 2003.

[8] N. Wiener. The homogeneous chaos. *American Journal of Mathematics*, 60(4):897–936, October 1938.

[9] M.M.R. Williams. Polynomial chaos functions and stochastic differential equations. *Annals of Nuclear Energy*, 33(9):774–785, June 2006.

[10] D. Xiu and J.S. Hesthaven. High-order collocation methods for differential equations with random inputs. *SIAM Journal on Scientific Computing*, 27(3):1118–1139, 2005.

[11] D. Xiu and G.E. Karniadakis. The wiener-askey polynomial chaos for stochastic differential equations. *SIAM Journal on Scientific Computing*, 24(2):619–644, 2002.